Serum tRNA-Derived Fragments as Potential Biomarkers in Children with Acute Intussusception

Wei Chen
Children's Hospital of Soochow University
Lian Zhao
Children's Hospital of Soochow University
Wan-liang Guo (gwlsuzhou@163.com)
Children's Hospital of Soochow University

Research article

Keywords: Pediatric, intussusception, Intestinal ischemia–reperfusion, Gene expression, Transfer ribonucleic acid (tRNA)–derived fragments

Posted Date: August 10th, 2020

DOI: https://doi.org/10.21203/rs.3.rs-50064/v1

Abstract

Background: The aim of the present study was to investigate whether transfer ribonucleic acid (tRNA)–derived fragments (tRFs) can serve as candidate biomarkers for pediatric intussusception.

Methods: Using high-throughput sequencing technology, we identified differentially expressed tRFs, and ultimately selected three tRFs to establish a signature as a predictive biomarker of pediatric intussusception. Selection of these three upregulated genes was verified using quantitative reverse-transcription polymerase chain reaction (qRT-PCR). We conducted receiver operator characteristic (ROC) curve analysis to evaluate the predictive accuracy of the selected genes for pediatric intussusception.

Results: We detected 732 tRFs and tRNA-derived stress-induced RNA (tiRNAs), 1705 micro-RNAs (miRNAs), 52 differentially expressed miRNAs, and 34 differentially expressed tRFs and tiRNAs between patients and controls. Compared with controls, we found 33 upregulated miRNAs, 24 upregulated tRFs and tiRNAs, 19 downregulated miRNAs, and 10 downregulated tRFs and tiRNAs in children with intussusception. Using qPCR, the expression trends of tRF-Leu-TAA-006, tRF-Gln-TTG-033 and tRF-Lys-TTT-028 were consistent with the sequencing results. AUCs of tRF-Leu-TAA-006, tRF-Gln-TTG-033 and tRF-Lys-TTT-028 were 0.984, 0.970 and 0.837, respectively.

Conclusion: Circulating tRF-Leu-TAA-006, tRF-Gln-TTG-033 and tRF-Lys-TTT-028 expression might be a novel potential biomarker for diagnosis of pediatric intussusception.

Introduction

Pediatric intussusception is one of the most common causes of bowel obstruction in the pediatric population. Affected children have one section of the intestine sliding into the adjacent section [1, 2]. Intestinal ischemia–reperfusion injury (I/R) can occur during pediatric intussusception [3, 4], and any delay in diagnosis or treatment can lead to loss of intestinal viability that requires bowel resection [5, 6].

In the clinical practice, the diagnosis of pediatric intussusception is mainly based on a combination of clinical symptoms and examinations from ultrasound (US) imaging, computed tomography (CT), or air enema [7]. Early detection of pediatric intussusception and associated intestinal I/R can improve prognosis and treatment efficacy [8, 9]. Until now, there has been no clinical biomarker for early diagnosis of pediatric intussusception and associated intestinal I/R.

Transfer ribonucleic acid (tRNA)–derived fragments (tRFs), a novel type of small non-coding RNA originating from tRNAs [10, 11], participate in many pathological processes [12]. These fragments can be released and detected in the peripheral circulation. Levels of tRFs can fluctuate in response to stimuli. Circulating levels of tRFs might be useful as the surrogate measurements of disease progression [13, 14]. However, there is no previous study that investigates the role of tRFs and tRNA-derived stress-induced RNA (tiRNAs) in pediatric intussusception and associated intestinal I/R. In the current study, we examined whether a gene expression profile could be used for early detection of pediatric intussusception.

Specifically, we conducted genome-wide transcriptional profiling using blood-derived tRFs and tiRNAs followed by real-time polymerase chain reaction (PCR) verification in children with intussusception.

Materials And Methods

1. Study subjects

We performed a cross-sectional study. The study protocol was approved by the Ethics Committee of the Children's Hospital of Soochow University, Suzhou, China (No. 20170506013). Written informed consent was obtained from their parents.

Demographic and clinical data were recorded for each study participant between August 1, 2019 and December 31, 2019 at the Children's Hospital of Soochow University. The diagnosis of intussusception was based on combined clinical symptom with the US examination. Once the diagnosis was made, air enema was performed as the treatment method.

2. RNA extraction

Peripheral blood samples was drawn right after the reduction of intussusception and mononuclear cells were isolated and then stored at − 80 °C for RNA extraction. We isolated total RNA using TRIzol Reagent (Invitrogen, Carlsbad, California, US) per the manufacturer's protocol.

3. Library preparation and tRF/tiRNA sequencing and data analysis

We used agarose electrophoresis to check the integrality of total RNA samples, and then quantified the samples using a NanoDrop ND-1000 Spectrophotometer (Thermo Scientific, Thermo Fisher Scientific, Waltham, Massachusetts, USA). In order to remove RNA modifications that interfere with small-RNA sequencing (RNA-seq) library construction, total RNA samples were first pretreated as follows: 3-aminoacyl (charged) deacylation to 3-OH for 3-adaptor ligation; 3-cP (2,3-cyclic phosphate) removal to 3-OH for 3-adaptor ligation; 5-OH (hydroxyl group) phosphorylation to 5-P for 5-adaptor ligation; and m1A and m3C demethylation for efficient reverse transcription. We took pretreated total RNA from each sample for tRF and tiRNA sequencing (tRF-seq, tiRNA-seq) library preparation. The procedures included (1) 3-adapter ligation; (2) 5-adapter ligation; (3) complementary deoxyribonucleic acid (cDNA) synthesis; (4) PCR amplification; and (5) size selection of ∼134–160-bp PCR amplified fragments (corresponding to ∼14–40-nt small RNAs). The completed libraries were quantified using an Agilent 2100 Bioanalyzer (Agilent Technologies, Inc., Santa Clara, California, US). We mixed the libraries in equal amounts according to the quantification results and used them for further sequencing.

We denatured DNA fragments in well-mixed libraries with 0.1 M NaOH to generate single-stranded DNA molecules and then loaded them onto the reagent cartridge at a concentration of 1.8 pM. The sequencing was performed on a NextSeq system using a NextSeq 500/550 V2 kit (#FC-404-2005; Illumina, Inc., San Diego, California, USA) per the manufacturer's instructions. We performed 50 cycles of sequencing.

We analyzed images and performed base calling using Solexa Pipeline v1.8 software (Off-Line Basecaller software v1.8; Illumina). Sequencing quality was examined using FastQC software [15]. We aligned trimmed reads (pass Illumina quality filter, trimmed 5,3-adaptor bases by cut adapt [16]), allowing for only one mismatch to mature tRNA sequences. Then, we aligned the reads that did not map using Bowtie software [17], allowing for only one mismatch to precursor tRNA sequences. The remaining reads were aligned using miRDeep2 software [18], allowing for only one mismatch to micro-RNA (miRNA) reference sequences. We were then able to calculate the expression profiling of tRFs, tiRNA, and miRNA based on counts of reads mapped. Differentially expressed tRFs, tiRNAs and miRNAs were screened based on count value using the edgeR package in R software [19]. We performed principal component analysis (PCA), correlation analysis, and hierarchical clustering to create pie, Venn, scatter, and volcano plots in an R or Perl environment for statistical computing and graphics of the expressed tRFs and tiRNAs. The functions and pathways of almost all tRFs were classified according to Gene Ontology (GO) assignment and the Kyoto Encyclopedia of Genes and Genomes (KEGG) database. We used Cytoscape software (version 3.8.0, https://cytoscape.org/) to predict the network of the top 100 potential targets of tRFs and tiRNAs.

4. Real-time quantitative reverse transcription polymerase chain reaction assay

Using qRT-PCR, we selected and quantified the upregulated expression of tRF-Leu-TAA-006, tRF-Gln-TTG-033, and tRF-Lys-TTT-028 in both study groups. We performed qPCR using a SYBR Green PCR Kit (Applied Biosystems, Foster City, California, USA) per the manufacturer's instructions. We normalized gene expression to β-actin messenger RNA (mRNA). Relative expression of the gene transcript was calculated using the $2^{-\Delta\Delta Ct}$ method.

5. Statistical analysis

We used SPSS software (version 20.0, IBM, Armonk, New York, USA) for statistical analysis. Continuous data are presented as mean ± standard deviation (SD). Inter-group comparisons were performed by the rank sum test. Receiver operator characteristic (ROC) curve analysis was conducted and the area under the ROC curve (AUC) was calculated to evaluate the diagnostic accuracy of selected genes in pediatric intussusception. A $P < 0.05$ was considered statistically significant.

Results

1. Demographic and clinical data

A total of 20 pediatric-intussusception patients and 20 healthy controls were included in the study. Patients' demographic and clinical data are summarized in Table 1. There was no statistically significant difference between the children with intussusception and healthy controls in terms of age and gender.

Table 1
Demographic and clinical data of pediatric intussusception

Patient No.	Pathological type	successful versus failed air enemas for intussusception	Mass location	Signs of plain radiography
1	Ileum colon	Success	hepatic flexure of colon	Quadrant gas-filled bowel loop
2	Ileum colon	Success	cecum	Paucity of bowel gas
3	Ileum colon	Success	transverse colon	Paucity of bowel gas
4	Ileum-ileum ,duplication of intestine	Failed, operative	hepatic flexure of colon	Distended bowel with a mass
5	Ileum colon	Success	hepatic flexure of colon	Quadrant gas-filled bowel loop
6	Ileum colon	Success	hepatic flexure of colon	Distended bowel with a mass
7	Ileum colon	Success	hepatic flexure of colon	Quadrant gas-filled bowel loop
8	Ileum cecum	Success	cecum	Distended bowel with a mass
9	Ileum colon	Success	hepatic flexure of colon	Paucity of bowel gas
10	Ileum colon	Success	hepatic flexure of colon	Quadrant gas-filled bowel loop
11	Ileum colon	Success	hepatic flexure of colon	Quadrant gas-filled bowel loop
12	Ileum cecum	Success	cecum	Quadrant gas-filled bowel loop
13	Ileum colon	Success	hepatic flexure of colon	Paucity of bowel gas
14	Ileum-ileum	Failed, operative	hepatic flexure of colon	Quadrant gas-filled bowel loop

Patient No.	Pathological type	successful versus failed air enemas for intussusception	Mass location	Signs of plain radiography
15	Ileum colon	Success	hepatic flexure of colon	Quadrant gas-filled bowel loop
16	Ileum colon	Success	hepatic flexure of colon	Quadrant gas-filled bowel loop
17	Ileum colon	Success	hepatic flexure of colon	Paucity of bowel gas
18	Ileum colon	Success	hepatic flexure of colon	Quadrant gas-filled bowel loop
19	Ileum colon	Success	hepatic flexure of colon	Quadrant gas-filled bowel loop
20	Ileum cecum	Success	cecum	Paucity of bowel gas

2. Differentially expressed serum tRF and tiRNA levels in patients and controls

In this study, we detected 732 tRFs and tiRNAs, 1705 miRNAs, 52 differentially expressed miRNAs, and 34 differentially expressed tRFs and tiRNAs between the two groups (Fig. 1A–B). We found nine types of tRFs and tiRNAs in both groups, including tRF-1, tRF-2, tRF-3a, tRF-3b, tRF-5a, tRF-5b, tRF-5c, tiRNA-3, and tiRNA-5 (Fig. 2A–C). As shown in Fig. 1A–B, compared with controls, patients had 33 upregulated miRNAs, 24 upregulated tRFs and tiRNAs, 19 downregulated miRNAs, and 10 downregulated tRFs and tiRNAs (fold change, cutoff 1.5; *P*-value, cutoff 0.05).

3. qRT-PCR validation

Next, in order to validate differential expression, we used qPCR to measure three high candidates, tRF-Leu-TAA-006, tRF-Gln-TTG-033, and tRF-Lys-TTT-028, in the 20 patient samples and 20 control samples. The results showed that the expression trend of these three tRFs was consistent with the sequencing results; the difference was statistically significant (Fig. 3).

4. Predictive value of specific tRFs and tiRNAs as diagnostic biomarkers of pediatric intussusception

ROC curves for differentiating between pediatric-intussusception patients and healthy controls were based on expression levels of tRF-Leu-TAA-006, tRF-Gln-TTG-033 and tRF-Lys-TTT-028. tRFs and tiRNAs

with AUC > 0.5 and $P < 0.05$ were considered appropriate biomarkers. The results showed that the AUCs of tRF-Leu-TAA-006, tRF-Gln-TTG-033 and tRF-Lys-TTT-028 were 0.984 (95% confidence interval [CI], 0.952–1.000; $P < 0.05$), 0.970 (95% CI, 0.933–1.000; $P < 0.05$) and 0.837 (95% CI, 0.722–0.951; $P < 0.05$), respectively (Fig. 4).

5. Prediction of potential targets for differentially expressed tRFs and tiRNAs and functional analysis of target genes

We performed GO and KEGG pathway analyses to analyze target genes in order to explore the potential functions and mechanisms of tRFs and tiRNAs in pediatric intussusception. Classification of tRF and tiRNA target genes was based on the Cellular Component (CC), Molecular Function (MF), and Biological Process (BP) categories. GO annotations demonstrated that the target genes of tRF-Gln-TTG-033 were abundant in the function of material metabolism, such as the nucleic acid metabolic process, heterocycle metabolic process, organonitrogen compound metabolic process, nitrogen compound metabolic process, and organic-substance metabolic process (Fig. 5A). In addition, the target genes of tRF-Gln-TTG-033 were primarily found in the organelle, intracellular compartment, and cell part, while the MFs of its products mainly included binding, protein binding, and transferase activity (Fig. 5B). After mapping the targeted genes of tRF-Gln-TTG-033 in the KEGG database, we found that these genes participated in the “AMPK signaling pathway”, “FoxO signaling pathway”, “Cellular senescence” and “Relaxin signaling pathway”, which were associated with I/R (Fig. 5C).

Regarding tRF-Leu-TAA-006, BP-based terms revealed that tRF target genes were related to the cellular protein modification process and the protein modification process (Fig. 6A). In addition, the target genes of tRF-Leu-TAA-006 were primarily found in the intracellular membrane-bounded organelle, intracellular compartment, and cell part; and the MFs of its products mainly included binding, protein binding and ion binding (Fig. 6B). After mapping the targeted genes of tRF-Leu-TAA-006 in the KEGG database, we found that these genes participated in the “RAS pathway” and “Protein procession”, which were associated with I/R (Fig. 6C).

For tRF-Lys-TTT-028, target genes played a role in lipid metabolic processes, including the nucleic acid metabolic process, macromolecule metabolic process, cellular macromolecule metabolic process, and RNA metabolic process (Fig. 7A). In addition, these genes were primarily found in the intracellular membrane-bounded organelle, intracellular part, and intracellular, and the MFs of its products mainly included DNA binding, heterocyclic compound binding, and organic cyclic-compound binding (Fig. 7B). After mapping the targeted genes of tRF-Lys-TTT-028 in the KEGG database, we found that these genes participated in “Signaling pathways regulating pluripotency of stem cells” and “Taurine and hypotaurine metabolism”, which were associated with I/R (Fig. 7C).

6. tRF–target gene interaction network analysis

Having revealed the correlation between tRFs and pediatric intussusception, we next explored interactions between target genes predicted by our biological analysis to better understand the intrinsic mechanisms

of tRFs. Using the Miranda (http://www.microrna.org/) and RNAhybrid (M. Rehmsmeier, 2004) tools, we found the top 100 potential targets of tRF-Leu-TAA-006, tRF-Gln-TTG-033, and tRF-Lys-TTT-028, as shown respectively in Figs. 8A, 8B and 8C.

Discussion

Intussusception is one of the most common causes of bowel obstruction in children. I/R in intussusception can result in mucosal erosion and hemorrhagic ulceration, as well as necrosis of the bowel, lung injury, and multiple-organ dysfunction syndrome [20]. Oxidative stress can play a crucial role in I/R in pediatric intussusception [21]. Early detection of intestinal I/R in intussusception can improve prognosis and reduce complications in the intestines and extraintestinal organs. Although many efforts have been made to identify biomarkers of pediatric intussusception and associated I/R, no definite biomarkers are currently available in clinical practice.

Non-coding RNAs (ncRNAs) can be released to circulate in the peripheral blood. Circulating levels of tRFs could be useful as biomarkers of some diseases and surrogate measures of disease progression [13, 14], indicating their potential use in diagnosis and assessment of I/R in pediatric intussusception. In our previous studies, we found I/R in both our animal models and our pediatric intussusception patients. Therefore, we decided to test the expression of tRFs in serum from patients and further focus on biological analysis to verify whether circulating tRFs could serve as potential biomarkers in pediatric intussusception and associated I/R.

In the present study, we first performed high-throughput sequencing (HTS) to detect the expression profiles of tRFs in pediatric intussusception patients. To validate differential expression in the sequencing data, we selected three dysregulated tRFs for qRT-PCR review to verify the authenticity of the profiles. We detected the most significantly upregulated tRFs—tRF-Leu-TAA-006, tRF-Gln-TTG-033, and tRF-Lys-TTT-028—in serum samples from patients. Our qRT-PCR results demonstrated that all three tRFs were significantly upregulated in patients compared with controls. Via GO analysis, we learned that the targeted genes of these differentially expressed tRFs were involved in metabolism, protein modification, binding, transferase activity, protein binding, DNA binding, heterocyclic compound binding, and organic cyclic-compound binding. In mapping all targeted genes to the KEGG database, we noted that they participated in the following: “AMPK signaling pathway”, “FoxO signaling pathway”, “Cellular senescence”, “Relaxin signaling pathway”, “RAS pathway”, “Protein procession”, “Signaling pathways regulating pluripotency of stem cells” and “Taurine and hypotaurine metabolism”. This is consistent with findings in the literature that these signaling pathways play important roles in I/R [17–22]. However, the involvement of these dysregulated tRFs and their target genes in I/R in the pediatric intussusception process via these signaling pathways require further studies.

To apply the expression values of serum tRFs and tiRNAs for clinical diagnosis, we analyzed the ROC curves. We found that serum tRF-Leu-TAA-006, tRF-Gln-TTG-033, and tRF-Lys-TTT-028 were significantly upregulated in pediatric intussusception children compared with controls. The results showed that AUCs

of tRF-Leu-TAA-006, tRF-Gln-TTG-033, and tRF-Lys-TTT-028 were 0.984, 0.970, and 0.837, respectively (Fig. 5). These findings suggested that serum levels of these three tRFs might be involved in the development of pediatric intussusception and could become new biomarkers for pediatric intussusception.

There are some limitations in the present study. First, the sample size was relatively small. Second, only three tRFs identified in microarray experiments were validated via qRT-PCR. Future studies should be conducted with larger sample sizes and in-depth verification of more candidate genes. Finally, the potential mechanisms of tRF-Leu-TAA-006, tRF-Gln-TTG-033, and tRF-Lys-TTT-028 in pediatric intussusception still require further studies.

In conclusion, the present study provided an overall analysis of tRFs and tiRNAs in pediatric intussusception and indicated that tRF-Leu-TAA-006, tRF-Gln-TTG-033, and tRF-Lys-TTT-028 could play important roles in pediatric intussusception. Results of further biological analysis suggested that these three tRFs could serve as novel serological biomarkers with significant accuracy in diagnosing pediatric intussusception. We believe that our research could offer clues for further research into the mechanism of tRFs in pediatric intussusception.

Abbreviations

tRNA = transfer ribonucleic acid; tRFs = transfer ribonucleic acid–derived fragments; qRT-PCR = quantitative reverse-transcription polymerase chain reaction; ROC = receiver operator characteristic; tiRNAs = transfer ribonucleic-derived stress-induced ribonucleic acids; miRNAs = micro- ribonucleic acids; I/R = ischemia–reperfusion injury; US = ultrasound; CT = computed tomography; RNA-seq = RNA sequencing; PCA = principal component analysis; GO = Gene Ontology; KEGG = Kyoto Encyclopedia of Genes and Genomes; mRNA = messenger RNA; CC = Cellular Component; MF = Molecular Function; BP = Biological Process; ncRNAs = Non-coding RNAs; HTS = high-throughput sequencing

Declarations

Ethics approval and consent to participate

The study protocol was approved by the Ethics Committee of the Children's Hospital of Soochow University, Suzhou, China (No. 20170506013).

Availability of data and materials

All data generated or analysed during this study are included in this article

Competing interests

The authors declare that they have no competing interests.

Funding

This work was supported by National Natural Science Foundation (No.81971685).

Authors' contributions

Study conception and design: WL G. Acquisition of data: WC, LZ. Analysis and interpretation of data: WL G. Drafting of manuscript: LZ, WC. Critical revision of manuscript: WL G. All authors have read and approved the manuscript.

Acknowledgements

Not applicable.

Authors' information

Department of Radiology, Children’s Hospital of Soochow University, Suzhou, China, 215025

References

1. Jiang J, Jiang B, Parashar U, Nguyen T, et al. Childhood intussusception: a literature review. PLoS One. 2013;8:e68482.
2. Guo WL, Hu ZC, Tan YL, et al. Risk factors for recurrent intussusception in children: a retrospective cohort study. BMJ Open. 2017;7:e018604.
3. Guo WL, Wang J, Liu C, et al. Expression of p38 mitogen-activated protein kinase (p38MAPK) and pathological change in intussusception. Pediatr Int. 2016;58:881–6.
4. Tan HZC, Huang YL. SG, et al. Molecular imaging of Toll-like receptor 4 detects ischemia-reperfusion injury during intussusception. Oncotarget. 2018;9:7882–90.
5. Hanquinet S, Anooshiravani M, Vunda A, et al. Reliability of color Doppler and power Doppler sonography in the evaluation of intussuscepted bowel viability. Pediatr Surg Int. 1998;13:360–2.
6. Guo WL, Wang J, Zhou M, et al. The role of plain radiography in assessing intussusception with vascular compromise in children. Arch Med Sci. 2011;7:877–81.
7. Carroll AG, Kavanagh RG, Ni Leidhin C, et al. Comparative Effectiveness of Imaging Modalities for the Diagnosis and Treatment of Intussusception: A Critically Appraised Topic. Acad Radiol. 2017;24:521–9.
8. Dörterler ME, Kocaman OH. Selection of Pneumatic Reduction in Invagination Treatment and the Factors Affecting the Success of This Method. Cureus. 2019;11:e5928.
9. McDermott VG, Taylor T, Mackenzie S, et al. Pneumatic reduction of intussusception: clinical experience and factors affecting outcome. Clin Radiol. 1994;49:30–4.
10. Soares AR, Santos M. Discovery and function of transfer RNA-derived fragments and their role in disease. Wiley Interdiscip Rev RNA. 2017; 8.

11. Shen L, Gan M, Tan Z, et al. A Novel Class of tRNA-Derived Small Non-Coding RNAs Respond to Myocardial Hypertrophy and Contribute to Intergenerational Inheritance. Biomolecules. 2018; 8.
12. Shen Y, Yu X, Zhu L, et al. Transfer RNA-derived fragments and tRNA halves: biogenesis, biological functions and their roles in diseases. J Mol Med (Berl). 2018;96:1167–76.
13. Huang Y, Ge H, Zheng M, et al. Serum tRNA-derived fragments (tRFs) as potential candidates for diagnosis of nontriple negative breast cancer. J Cell Physiol. 2020;235:2809–24.
14. Tosar JP, Cayota A. Extracellular tRNAs and tRNA-derived fragments. RNA Biol. 2020;19:1–19.
15. Andrews S. Babraham Bioinformatics - FastQC A Quality Control tool for High Throughput Sequence Data. Soil. 1973;5:47–81.
16. Martin M. CUTADAPT removes adapter sequences from high-throughput sequencing reads. EMBnetjournal. 2011;17:10–2.
17. Langmead B, Trapnell C, Pop M, et al. Ultrafast and memory-efficient alignment of short DNA sequences to the human genome. Genome Biol. 2009;10:R25.
18. Friedländer MR, Mackowiak SD, Li N, et al. miRDeep2 accurately identifies known and hundreds of novel microRNA genes in seven animal clades. Nucleic Acids Res. 2012;40:37–52.
19. Robinson MD, McCarthy DJ, Smyth GK. edgeR: a Bioconductor package for differential expression analysis of digital gene expression data. Bioinformatics. 2010;26:139–40.
20. Pierro A, Eaton S. Intestinal ischemia reperfusion injury and multisystem organ failure. Semin Pediatr Surg. 2004;13:11–7.
21. Wu MJ, Chen M, Sang S, et al. Protective effects of hydrogen rich water on the intestinal ischemia/reperfusion injury due to intestinal intussusception in a rat model. Med Gas Res. 2017;7:101–6.
22. Liu Z, Chen JM, Huang H, et al. The protective effect of trimetazidine on myocardial ischemia/reperfusion injury through activating AMPK and ERK signaling pathway. Metabolism. 2016;65:122–30.
23. Clements ME, Chaber CJ, Ledbetter SR, et al. Increased cellular senescence and vascular rarefaction exacerbate the progression of kidney fibrosis in aged mice following transient ischemic injury. PLoS One. 2013;8:e70464.
24. Juhasz B, Thirunavukkarasu M, Pant R, et al. Bromelain induces cardioprotection against ischemia-reperfusion injury through Akt/FOXO pathway in rat myocardium. Am J Physiol Heart Circ Physiol. 2008;294:H1365–70.
25. Pando R, Cheporko Y, Haklai R, et al. Ras inhibition attenuates myocardial ischemia-reperfusion injury. Biochem Pharmacol. 2009;77:1593–601.
26. Liu H, Wang L, Weng X, et al. Inhibition of Brd4 alleviates renal ischemia/reperfusion injury-induced apoptosis and endoplasmic reticulum stress by blocking FoxO4-mediated oxidative stress. Redox Biol. 2019;24:101195.

27. Jouret F, Leenders J, Poma L, et al. Nuclear Magnetic Resonance Metabolomic Profiling of Mouse Kidney, Urine and Serum Following Renal Ischemia/Reperfusion Injury. PLoS One. 2016;11:e0163021.
28. Zhang P, Ming Y, Cheng K, et al. Gene Expression Profiling in Ischemic Postconditioning to Alleviate Mouse Liver Ischemia/Reperfusion Injury. Int J Med Sci. 2019;16:343–54.
29. Valle Raleigh J, Mauro AG, Devarakonda T, et al. Reperfusion therapy with recombinant human relaxin-2 (Serelaxin) attenuates myocardial infarct size and NLRP3 inflammasome following ischemia/reperfusion injury via eNOS-dependent mechanism. Cardiovasc Res. 2017;113:609–19.

Figures

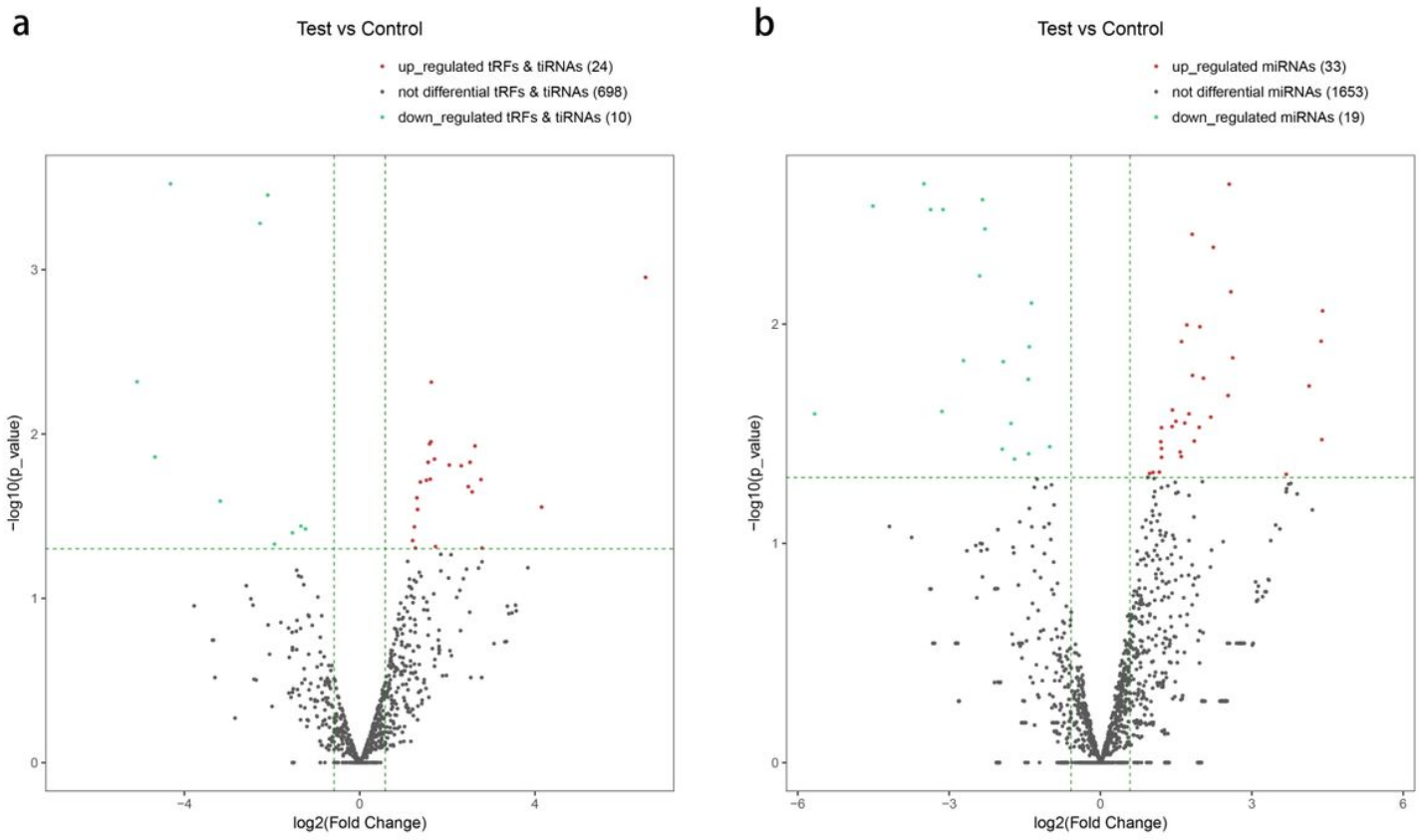

Figure 1

Differentially expressed tRFs (A) and miRNAs (B) between pediatric intussusception patients and healthy controls.

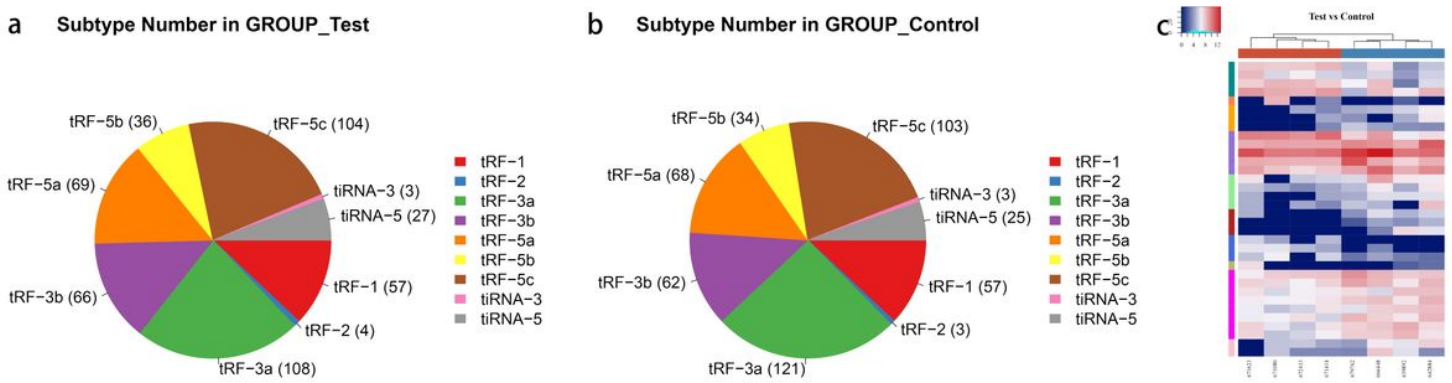

Figure 2

Subtypes of tRFs (A) and tiRNAs (B) in patients and controls.

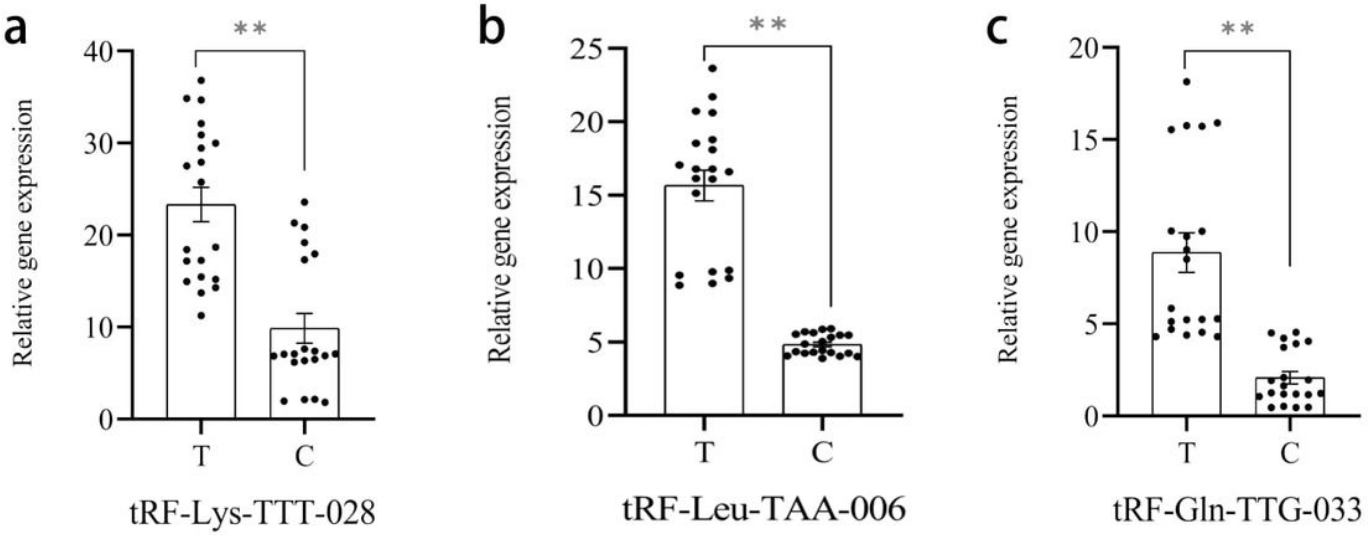

Figure 3

Verification of differentially expressed tRFs between patients and controls using qRT-PCR.

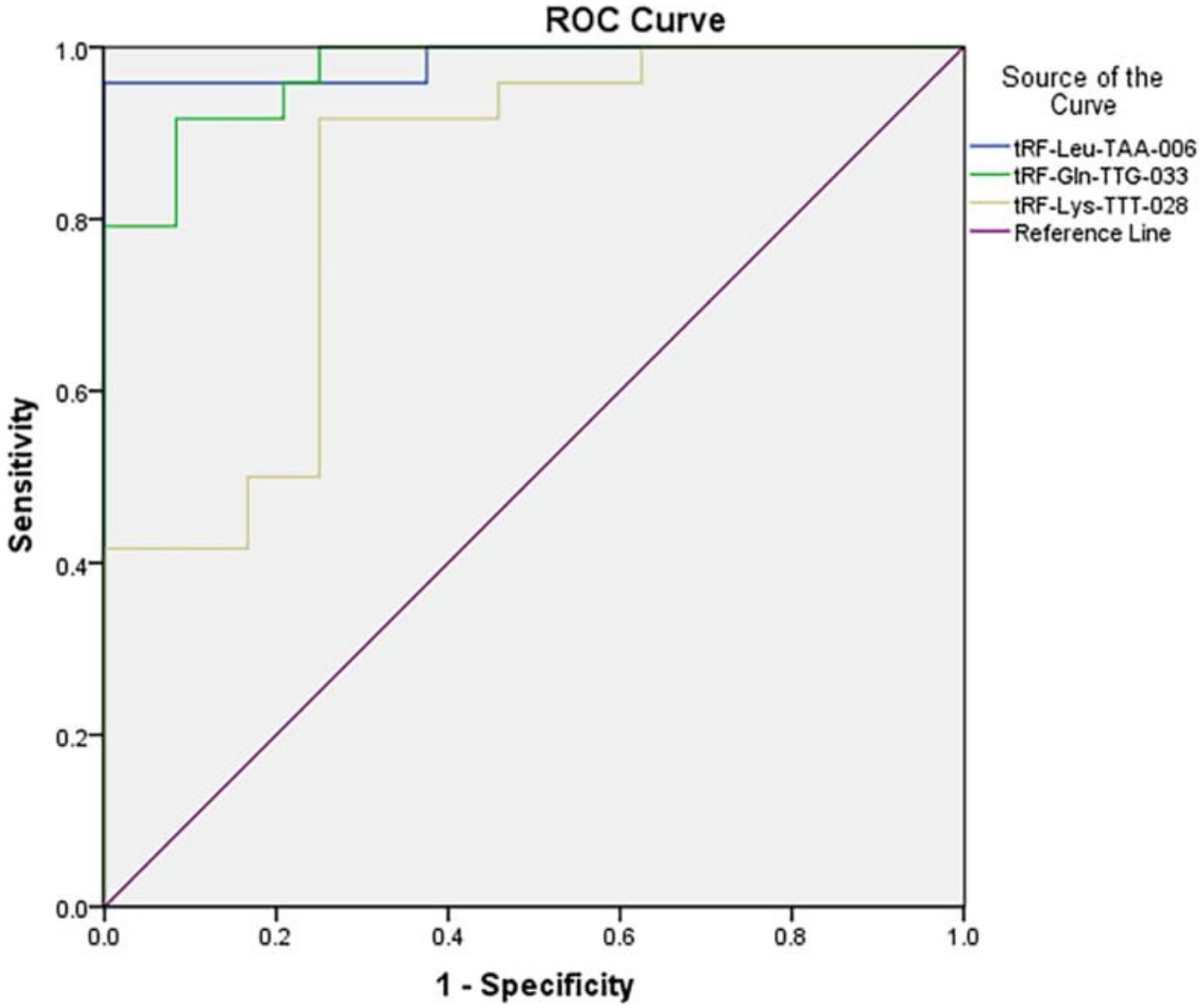

Figure 4

ROC curves of three differentially expressed tRFs between patients and controls.

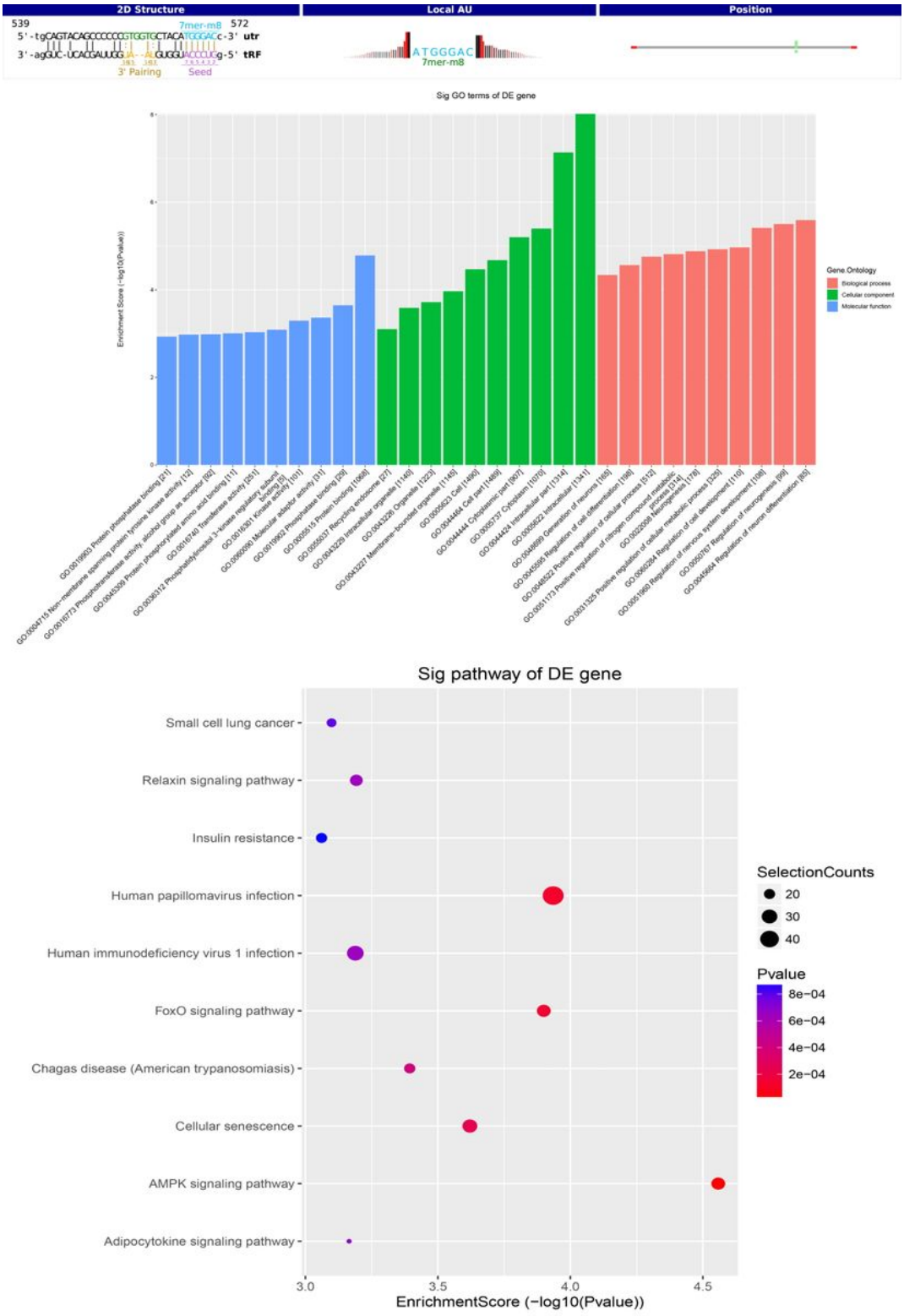

Figure 5

GO and pathway analysis of tRF-Gln-TTG-033. Target genes were predicted by Miranda algorithms and TargetScan miRNA prediction programs.

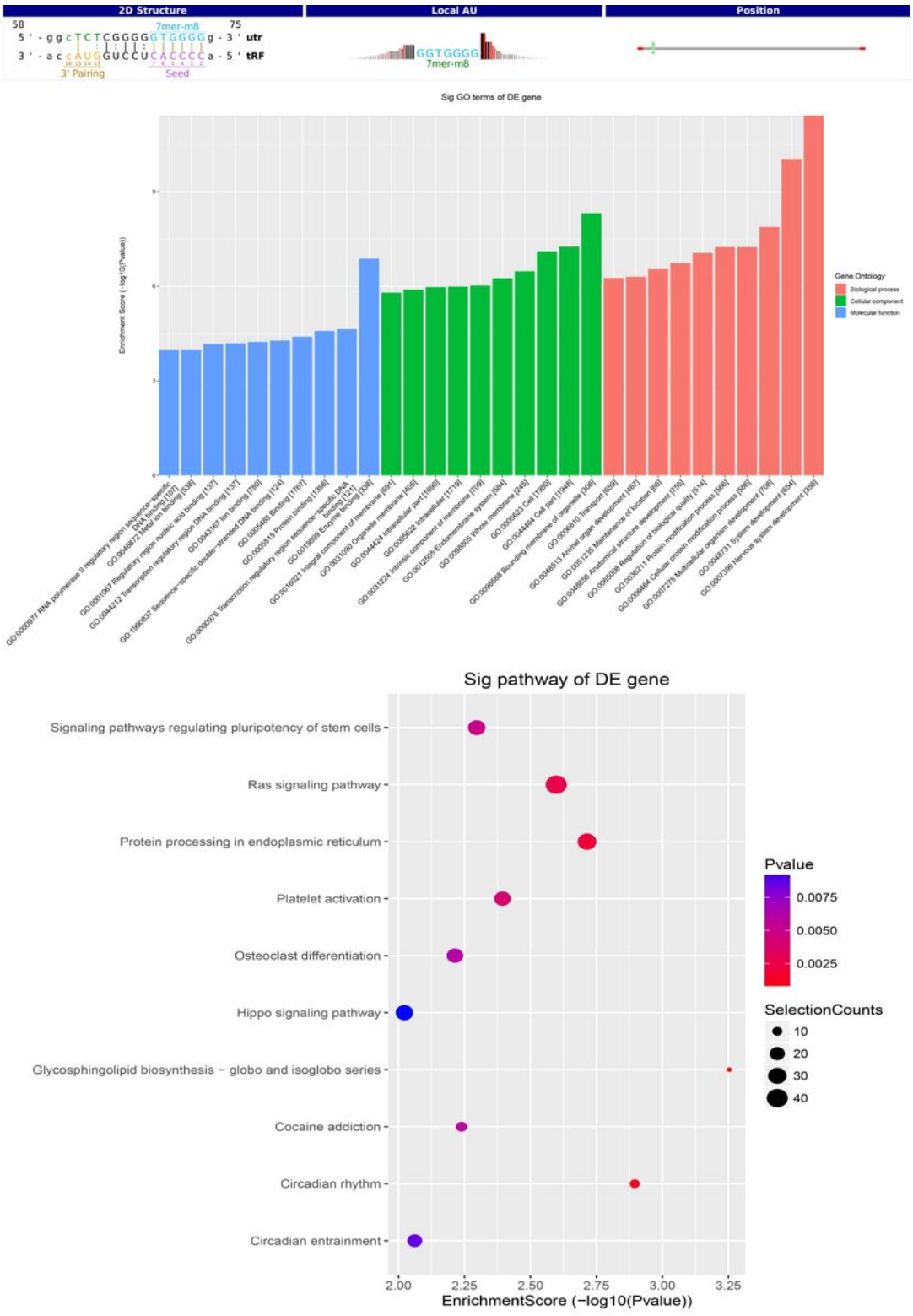

Figure 6

GO and pathway analysis of tRF-Leu-TAA-006. Target genes were predicted by Miranda algorithms and TargetScan miRNA prediction programs.

Figure 7

GO and pathway analysis of tRF-Lys-TTT-028. Target genes were predicted by Miranda algorithms and TargetScan miRNA prediction programs.

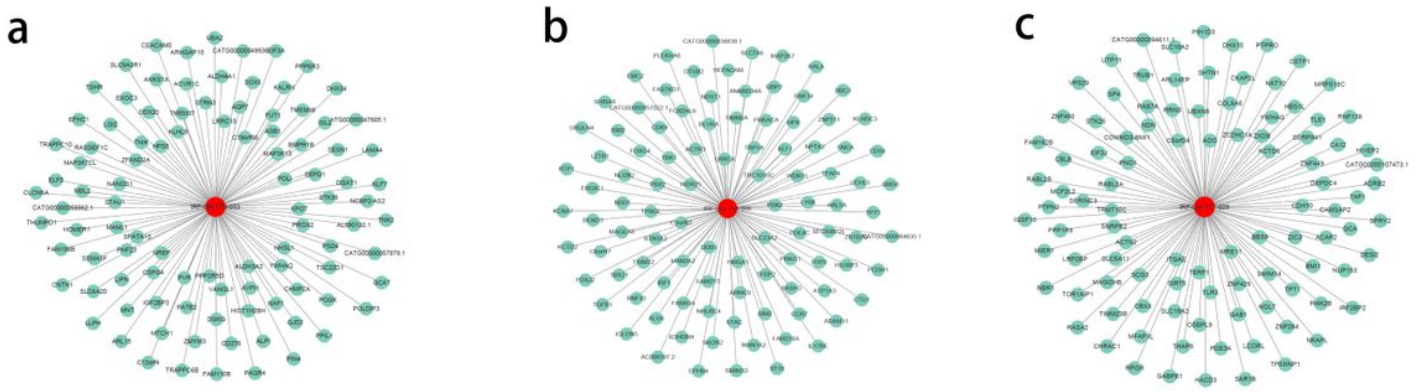

Figure 8

Top 100 potential targets of tRF-Leu-TAA-006 (A), tRF-Gln-TTG-033 (B) and tRF-Lys-TTT-028 (C).